Predictions in Ungauged Basins: PUB Kick-off (Proceedings of the PUB Kick-off meeting held in Brasilia, 20–22 November 2002). IAHS Publ. 309, 2007.

The generation of synthetic brightness temperature images to improve rainfall estimation from GOES satellite

DANIEL F. BARRERA

Departamento de Ciencias de la Atmósfera y los Océanos- FCEN,
Universidad de Buenos Aires / CONICET, Ciudad Universitaria, 1428 Buenos Aires, Argentina
barrera@at.fcen.uba.ar

Abstract The "auto-estimator" technique (Vicente *et al.*, 1998) was applied to estimate rain intensity from GOES IR images. It is based on an empirically adjusted power-law function relating the cloud top temperature (computed from infrared outgoing radiation in the spectral channel of 10.7 μ wavelength measured at the satellite) to the volumetric rain intensity estimated from radar echoes at the cloud base. Accumulated precipitation is then obtained by integration in time, assuming constant rain intensity at each pixel during the lapse assigned to the analysed image, as if the evolution of cloud systems was stopped along such a lapse. For the USA and surroundings (where this technique was originally applied) the GOES-E and GOES-W satellites provide images every 15 mins, which is then the lapse of integration in normal operation. Because of the movement of cloud systems (and raining cells) over the terrain, the assumption of constant rain intensity causes a deformation in the obtained rainfall fields, with artificially enhanced maximum centres at the centre sites captured by the images. When images are separated in longer time lapses, the mentioned deformation becomes more important. This is the case for Central and South America, where GOES-E makes a complete scan every 30 mins in normal operation, that is about the period of the life cycle of a convective cell. To better describe the displacement of cloud systems and minimize the mentioned deformation, the generation of synthetic brightness temperature images interpolated in time between two consecutive observed images was proposed. The displacement of cloud systems and the vertical evolution of cloud tops were taken into account for interpolations in space and time. The region covered by the working images was divided into boxes to take into account the natural evolution of cloud systems. In order to determine the mean vector displacement of cloud systems on each box, two criteria were proposed, applied and tested. The vector difference (in pixel units) between the analysed and the precedent images was searched, which complies with one of the following conditions: (1) the maximum cross-correlation coefficient of temperature values at pixels in two consecutive images; (2) the highest joint frequency of the same interval class of temperature (or same atmospheric layer) at pixels in two consecutive images. For testing the efficiency of both methods, the evolution of the temperature cloud shield for the following isotherms was analysed: 241ºK, 221ºK and 201ºK, which are the respective limits for significant, intense, and extreme precipitation intensity from convective clouds. Analysed cases were sequences of synthetic images bounded by observed consecutive images. The second criteria yielded more stable results when varying the number of boxes (the size of sectors). The most adequate box size was about 4º in latitude and longitude. The resulting isotherms showed very little changes when raising the bottom of the tropospheric driving layer from 268ºK to 248ºK temperature levels to account for the displacement of cloud systems.

Key words brightness temperature; precipitation estimation; synthetic images

INTRODUCTION

Precipitation estimates obtained from remote sensing data are in many cases the best or the only choice to initialize hydrological rainfall–runoff models. Even when the studied watershed has a pluviograph network, but is equipped with too few instruments to account for the spatial rainfall variability in the atmospheric mesoscale (Huff, 1970), rainfall estimates based on remotely sensed data are in most cases more adequate.

Because of the abovementioned variability, techniques of obtaining areal rainfall estimates from point measurements give results strongly affected by errors in most cases (Horton, 1923; Lebel *et al.*, 1987).

On the other hand, adequate remote sensing methods provide full spatial coverage, and even when rainfall estimates at a single pixel are not precise they introduce smaller errors in area-averaged estimations over sub-basins.

Several authors showed that microwave sensors mounted on low-orbit satellites provide information of cloud physics that infrared (IR) and visible radiometers cannot; therefore, rain rates obtained using microwave techniques (Vicente & Anderson, 1993; Viltard *et al.*, 1998; Miller *et al.*, 2000) are better estimates than the ones obtained from visible and IR data (Adler & Negri, 1988; Vicente *et al.*, 1998). However, infrared-based techniques based on data from geostationary satellites (which do not have microwave sensors) proved to be the best for estimating accumulated rainfall due to the frequent images that these satellites provide, which allow them to account for the temporal variability of rain.

In a former work (Barrera *et al.*, 2001) the "auto-estimator" (AE) technique (Vicente *et al.*, 1998) was applied to estimates of rain intensity from GOES IR images. It is based on an empirically adjusted power-law function relating the cloud top brightness temperature (computed from infrared outgoing radiation in the spectral channel of 10.7 μ wavelength measured at the satellite) and the volumetric rain intensity estimated from radar echoes at the cloud base over the area of the analysed pixel. After applying a correction factor related to tropospheric humidity and a "rain–no rain" mask accounting for the life cycle of a convective cell or a multi-cellular system, a rain rate value is estimated for each pixel of the image. Accumulated precipitation is then obtained by integration in time assuming constant rain intensity at each pixel during the lapse assigned to the analysed image, as if the evolution of cloud systems was stopped along such a lapse.

For the USA and surroundings (where this technique was originally applied) the GOES-E (for East) and GOES-W (for West) satellites provide images every 15 mins, which is then the lapse of integration in normal operation. Because of the movement of cloud systems (and raining cells) over the terrain, the assumption of constant rain intensity causes a deformation in the obtained rainfall fields, with artificially enhanced maximum centres at the centre sites captured by the images.

When images are less frequent and therefore separated by longer lapses, the mentioned deformation becomes more important. This is the case for Central and South America. In normal operation, GOES-E makes a complete scan of the designated Southern Hemisphere sector every 30 mins, except when a full disk scan is performed (every three hours) which causes the skipping of one or two consecutive Southern Hemisphere images. An example of two consecutive images is showed in Fig. 1.

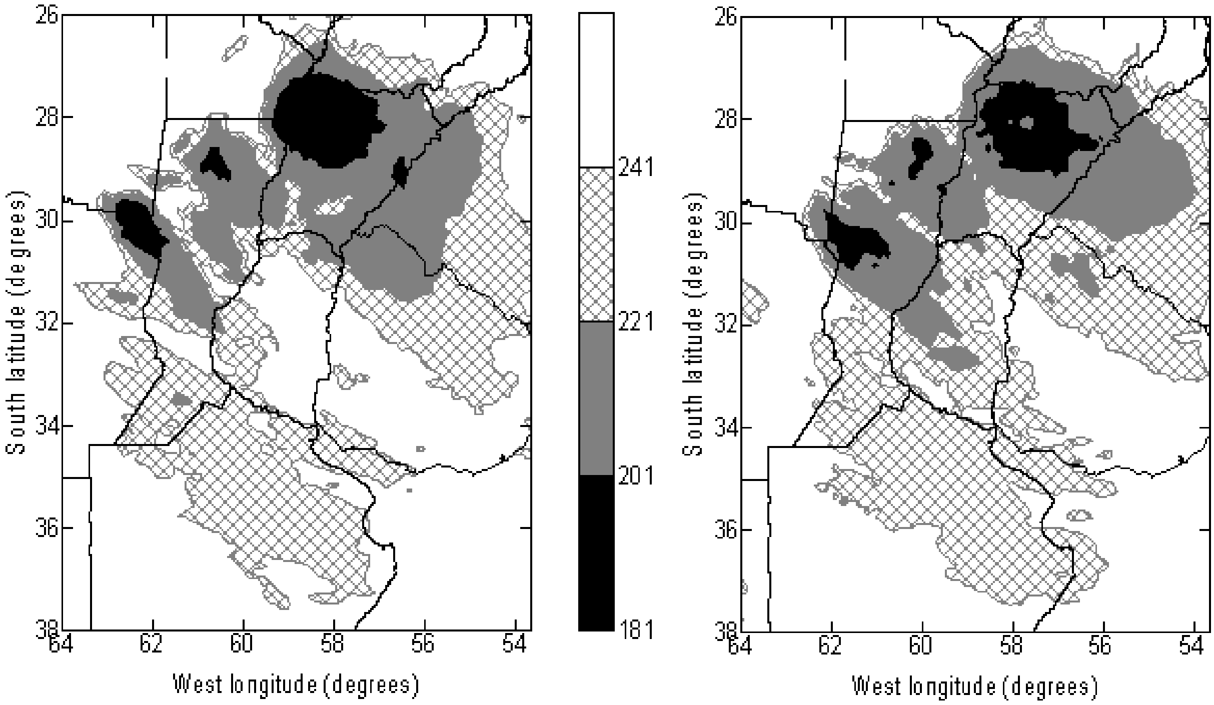

Fig. 1 Bright temperature fields from two consecutive GOES IR images. Class interval limits are degrees Kelvin. Date: 10 April 2002; Left 11.45 UTC; Right: 13.09 UTC.

METHODOLOGY

Proposed strategy

To better describe the displacement of cloud systems and minimize the above mentioned deformation in the obtained rainfall fields, the generation of synthetic brightness temperature images interpolated in time between two consecutive observed images was proposed.

The displacement of cloud systems and the vertical evolution of cloud tops were taken into account for interpolations in space and time.

Determination of displacement of cloud systems

The region covered by the working images was divided into boxes to take into account the natural variations of the mean movement of cloud systems from one region to another. In order to determine the mean vector displacement of cloud systems on each box, two criteria were proposed, applied and tested. The vector difference (in pixel units) between the analysed and the precedent images was searched, which complies with one of the following conditions:

– the maximum cross-correlation coefficient of temperature values at pixels in two consecutive images; and
– the highest joint frequency of the same interval class of temperature (or same atmospheric layer) at pixels in two consecutive images.

Election of the lapse between two consecutive synthetic images

Considering that most GOES-E images are due every 30 mins, a lapse of 10 mins (sub-multiple of 30) was designated to separate synthetic interpolated images. In this way a sequence of images every 10 mins is available when taking both observed and synthetic ones.

There are other reasons to generate at least one synthetic image every 10 min. The displacement velocity of raining clouds in meso-scale systems (driven by mid-tropospheric winds) is typically less than 60 km h^{-1}; therefore, clouds normally move less than 10 km in 10 min. Since the horizontal extension of a multi-cellular cloud is in the order of 10 km in diameter, having one image every 10 min gives the minimum frequency to capture the typical continuous trace of rain over the terrain during the life cycle of the cloud.

Also, because of the abovementioned typical velocities and dimensions, the assignment of a 10-min integration lapse to each image will allow the avoidance of significant over-estimations of maximum rainfall values, i.e. artificially enhanced maximum centres at the centre sites captured by the images, which would appear if rainfall was estimated from only observed images.

Since the actual cloud top evolution of a multi-cellular convective cloud during the lapse between two consecutive observed images is unknown, and because the life cycle of such cloud lasts typically about one hour, the cloud top bright temperature was assumed to vary linearly between two consecutive observed images.

More frequent synthetic images, such as one every 5 min, will yield better estimations of accumulated rainfall field, but will demand much more computing time.

DESIGNED EXPERIMENT AND RESULTS

Displacement of cloud systems

For testing the efficiency of both methods, the evolution of the temperature cloud shield for the following isotherms was analysed: 241ºK, 221ºK and 201ºK, which are the respective limits for significant, intense and extreme precipitation intensity from convective clouds. Analysed cases were sequences of synthetic images bounded by observed consecutive images.

The second criteria yielded more stable results when varying the number of boxes (the size of sectors). The most adequate size of boxes was about 4º in latitude and longitude; smaller boxes would allow a better description of the movement of cloud systems, but frequently would not permit adequate sample sizes of joint frequencies. A case study is shown in Figs 2, 3 and 4.

The resulting isotherms showed very little change when raising the bottom of the tropospheric driving layer from 268ºK to 248ºK temperature levels to account for the displacement of cloud systems.

Resulting rainfall estimates

Rainfall fields obtained by procedures 1 and 2 for a 3-hour period are shown in Fig. 5.

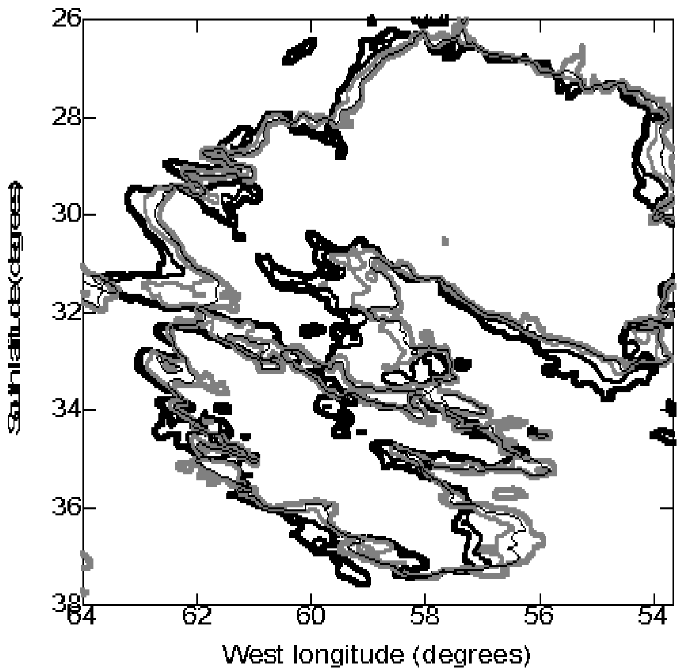

Fig. 2 241K cloud shield evolution from observed and synthetic images. Date: 10 April 2002; Observed: thick black, 11.45 UTC; thick grey, 13.09 UTC. Synthetic: medium black, 12.07 UTC; medium grey, 12.28 UTC; thin black, 12.48 UTC.

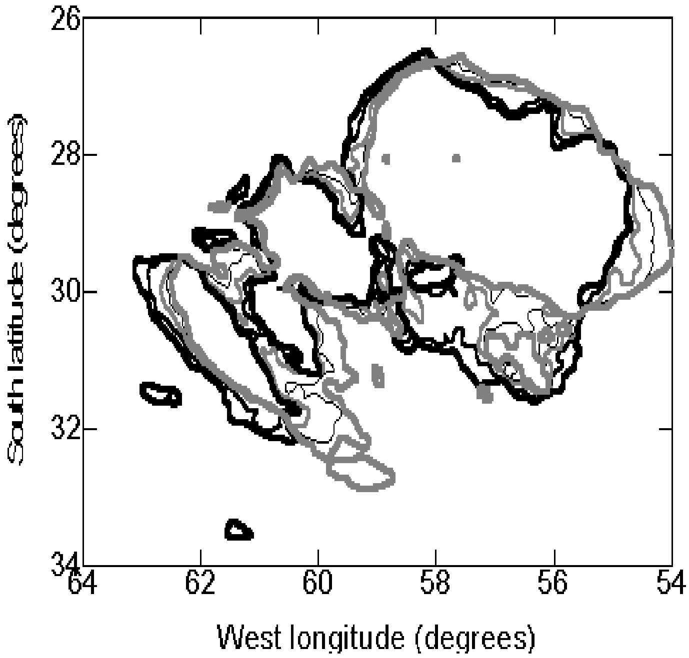

Fig. 3 221K cloud shield evolution from observed and synthetic images. Date: 10 April 2002; observed: thick black, 11.45 UTC; thick grey, 13.09 UTC. Synthetic: medium black, 12.07 UTC; medium grey, 12.28 UTC; thin black, 12.48 UTC.

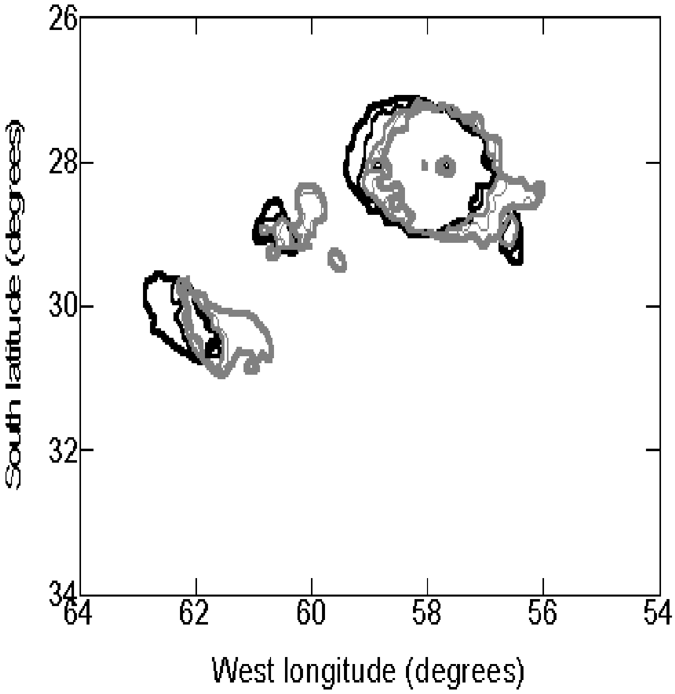

Fig. 4 201K cloud shield evolution from observed and synthetic images. Date: 10 April 2002; observed: thick black, 11.45 UTC; thick grey, 13.09 UTC. Synthetic: medium black, 12.07 UTC; medium grey, 12.28 UTC; thin black, 12.48 UTC.

Seven GOES IR images were available for the estimation of the precipitation field from 12 UTC to 15 UTC on 10 April 2002. In order to integrate computed values of rain intensity, lapses of, at most, 20 min before and after each image were assigned to it. In this way, a total period of 122 min out of 180 was covered by images when following procedure 1. A pro rata factor equal to 180/122 was applied to the obtained precipitation values at each pixel to account for the period of 58 min not represented by the available images. When applying procedure 2, 20 images were available (7 observed and 13 synthetic) covering the entire period of 180 min.

The main differences between the fields got by both procedures are:

– Contours are sharper in Fig. 5(a). In Fig. 5(b) the displacement of cloud systems leads to a smoothing of such contours.
– Centres of maximum and minimum values appear incorrectly enhanced in Fig. 5(a) because of the too long lapses assigned to the observed images.

The shape of the area with maximum values in Fig. 5(a) follow the shape of the cloud top isotherms at 13.09 UTC (which are elongated with an axis northwest–southeast) (see Fig. 1) because the lapse assigned to this image was the greater one (since the preceding image was taken at 11.45 UTC). On the other hand, in Fig. 5(b) the shape of the area with maximum values was delineated by the displacement of the cloud systems (from west northwest to east southeast), as it is seen in Figs 2, 3 and 4 from the evolution of isotherms. This effect is clearly evident for the centre of maximum rainfall on the west side of the sector located at approximately 61.2º west and 30.5º south.

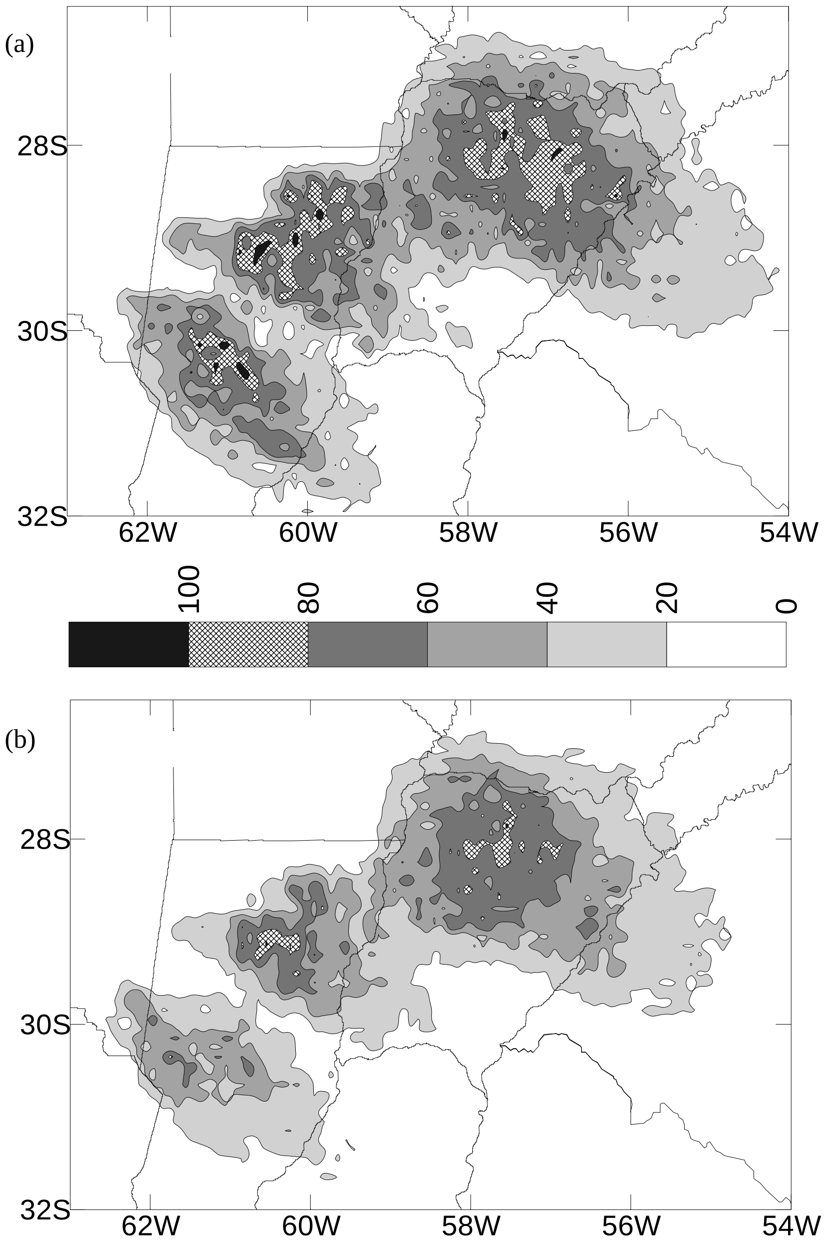

Fig. 5 Rainfall estimates on 10 April 2002 from 12 UTC to 15 UTC. (a) Procedure 1. (b) Procedure 2.

CONCLUSIONS

- The generation of synthetic bright temperature images proved to be an adequate way to increase the frequency of images and therefore to better describe the evolution of cloud systems from "instantaneous" images obtained by a geostationary satellite.
- Looking for the highest joint frequency of the same interval class of temperature (or same atmospheric layer) at pixels in two consecutive images has been found to be an efficient procedure to determine the mean displacement of thick clouds able to produce rain.

– Rainfall fields obtained with and without interpolation of synthetic images showed significant differences.

Acknowledgements This work was partially supported by Grant no 07-9743 of Agencia Nacional de Promoción Científica y Tecnológica. GOES-E images and gridded meteorological fields were provided by Servicio Meteorológico Nacional.

REFERENCES

Adler, R. & Negri, A. (1988) A satellite infrared technique to estimate tropical convective and stratiform rainfall. *J. App. Meteorol.* **27**, 30–51.

Barrera, D., Marcuzzi, E. & Naumann, G. (2001) Desarrollo del software de un Sistema Operativo de estimación de precipitación a partir de imágenes GOES. In: *IX Congreso Latinoamericano e Ibérico de Meteorología* (Buenos Aires, Argentina, 5–9 May 2001).

Horton, R. E. (1923) Accuracy of areal rainfall estimates. *Mon. Weather Rev*. **51**, 348–353.

Huff, F. A. (1970) Spatial distribution of rainfall rates. *Water Resour. Res.* **6**(1), 254–260.

Lebel, T., Bastin, G., Obled, C. & Creutin, J. D. (1987) On the accuracy of areal rainfall estimation: A case study. *Water Resour. Res.* **23**(11), 2123–2134.

Miller, S. D., Stephens, G. L., Drummond, C. K., Heidinger, A. K. & Partain, P. T. (2000) A multisensor dignostic satellite cloud property retrieval scheme. *J. Geophys. Res.* **105**, 19955–19971.

Vicente, G. & Anderson, J. (1993) Retrieval of rain rates from the combination of passive microwave radiometric measurements and infrared measurements. In: *20th Conf. Hurricane and Tropical Meteorology*, 151–154 (Amer. Meteor. Soc., San Antonio, Texas, 10–14 May 1993).

Vicente, G., Scofield, R. & Menzel, P. (1998) The operational GOES infrared rainfall estimation technique. *Bull. Am. Meteorol. Soc.* **79**, 1883–1898.

Viltard, N., Kummerow, C., Hong, Y. & Olson, S. (1998). Retrieval of precipitation from satellite passive microwave data using a physical/statistical approach in the context of TRMM. In: *9th Conference on Satellite Meteorology and Oceanography*, 509–512 (Amer. Meteor. Soc., Paris, France, 25–29 May 1998).